Competition between radiation and photofragmentation in the Ã 2 Σ + state of the SH/D rare gas complexes

Brian E. Applegate, Min-Chieh Yang, and Terry A. Miller

Citation: The Journal of Chemical Physics **109**, 162 (1998); doi: 10.1063/1.476545
View online: http://dx.doi.org/10.1063/1.476545
View Table of Contents: http://scitation.aip.org/content/aip/journal/jcp/109/1?ver=pdfcov
Published by the AIP Publishing

Articles you may be interested in

Rotational spectrum of SO3 and theoretical evidence for the formation of sixfold rotational energy-level clusters in its vibrational ground state
J. Chem. Phys. **140**, 244316 (2014); 10.1063/1.4882865

Microwave and ab initio studies of rare gas–methane van der Waals complexes
J. Chem. Phys. **120**, 9047 (2004); 10.1063/1.1691743

Radiative and predissociative lifetimes of the A 2 Σ + state (v ′ =0,1) of SH and SD: A highly correlated theoretical investigation
J. Chem. Phys. **115**, 2178 (2001); 10.1063/1.1381577

Theoretical investigations of the lifetime of SH and SD (Ã 2 Σ +) in MSH/D (M=Ne,Ar,Kr) complexes
J. Chem. Phys. **109**, 170 (1998); 10.1063/1.476546

Unimolecular reactions in the gas and liquid phases: A possible resolution to the puzzles of the trans-stilbene isomerization
J. Chem. Phys. **107**, 812 (1997); 10.1063/1.474381

This article is copyrighted as indicated in the article. Reuse of AIP content is subject to the terms at: http://scitation.aip.org/termsconditions. Downloaded to IP: 193.0.65.67 On: Sat, 29 Nov 2014 12:28:31

Competition between radiation and photofragmentation in the $\tilde{A}\ ^2\Sigma^+$ state of the SH/D rare gas complexes

Brian E. Applegate, Min-Chieh Yang, and Terry A. Miller
Laser Spectroscopy Facility, Department of Chemistry, The Ohio State University, Columbus, Ohio 43210

(Received 6 January 1998; accepted 25 March 1998)

The natural lifetimes of a large number of the vibrational levels of the excited $\tilde{A}\ ^2\Sigma^+$ electronic state of the family of rare gas complexes, R·SH (R=Ne, Ar, and Kr) and their deuterides, are reported. It is well known that the natural lifetime of the $\tilde{A}\ ^2\Sigma^+$ state of isolated SH/D is markedly shortened by a photofragmentation process. Our results for the complexes show that the rare gas atom plays an important role in inhibiting this process. From a classical model of the molecular system we are able to explain the trends observed in our lifetime data. The data from the R·SD complexes where for some vibrational levels the deuterium atom appears to be trapped between the rare gas and sulfur atoms allows us to establish a radiative lifetime for these complexes and the SH/D monomer. © *1998 American Institute of Physics.* [S0021-9606(98)00925-8]

I. INTRODUCTION

The dynamics of bond breaking in excited vibrational and/or electronic states of molecules lies at the heart of chemistry. As such, it is a subject that has been actively investigated for many years. However recent advances, both experimental[1–6] and computational,[7–9] have allowed an ever better understanding of these processes.

Typically one of the barriers to the understanding of the dynamical processes in molecules is a lack of knowledge about the potential energy surface(s) upon which these processes evolve. The $\tilde{A}\ ^2\Sigma^+$ state of the R·SH/D (R=Ne, Ar, Kr) complexes represent a case where the potential surface is rather well characterized. We have recently conducted a series of spectroscopic experiments[10] that measured the energies and rotational constants of well over 100 rotational levels of the R·SH/D $\tilde{A}\ ^2\Sigma^+$ state. These data have been used[11] to construct empirical potential surfaces that well reproduce the spectroscopic data. These surfaces represent an ideal starting point for the study of dynamics.

The isolated SH/D radical undergoes photochemical bond fission when excited to the $v=0$ level of the $\tilde{A}\ ^2\Sigma^+$ state. This process has been well studied with values for the natural lifetimes, τ_{nat}, being determined for both the SH (Refs. 12–14) and SD (Refs. 13–15) isotopomers. Recent studies[16–22] have shown that the presence of an inert gas atom can markedly retard the photofragmentation process of the diatomic moiety in a complex. Similarly we recently reported[23] that the τ_{nat} for Ar·SH could be more than a factor of 100 longer than free SH. Soon thereafter Aparkian *et al.*[24] reported that Kr or Ar matrices appeared to completely arrest the photofragmentation process in SH.

In this paper we report a detailed study of the competition between radiation and photofragmentation for $\tilde{A}\ ^2\Sigma^+$ SH/D as a function of vibrational level of the R·SH/D complex by determining the natural lifetimes of these states. Qualitatively such experimental data represent a measure of the efficiency of S–H/D bond fission as a function of the position on the excited state potential where the molecule is placed. In a companion paper,[25] McCoy has undertaken a detailed calculation of the dynamics upon this surface. In this paper we use portions of her results, based upon a simplified model of the dynamics, to rationalize our experimental results.

II. EXPERIMENT

The experimental apparatus (Fig. 1) used to acquire the lifetime data will be briefly described here. An excimer (Lumonics 500) laser operating at 193 nm (ArF) was focused with a 75 cm quartz lens into the vacuum chamber and used to photolyze the precursor gas approximately 1–2 mm after exiting a 500 μm orifice of a pulsed valve (General Valve). Approximately 25 mm downstream from the pulsed valve a Nd:YAG (Quanta-Ray DCR II) pumped dye laser (Quanta-Ray PDL II) with DCM laser dye (Exciton) was frequency doubled with a KDP crystal and used to pump the $\tilde{A}\ ^2\Sigma^+ - \tilde{X}\ ^2\Pi$ transition. The light was collected with a 2 in. f1 lens and projected on to the active area of a photomultiplier tube (PMT) (EMI 9659B). The signal from the PMT was passed through a preamplifier before being fed into a 175 MHz digital oscilloscope (Lecroy 9400a). Each temporal decay was averaged over 1000 shots on the oscilloscope and then sent over a GPIB interface to the experimental computer for analysis. Additionally the experimental computer was used to remotely scan the dye laser and control the digital oscilloscope.

The precursor for this experiment consisted of a mixture of 1% H_2S balance He (Matheson) gas combined with the appropriate rare gas, Ne, Ar, or Kr (AGA gas) to produce the desired complex. Alternatively for the deuteride complexes 1% D_2S, balance He, (Isotek) was used. In the case of the ^{1}H species additional He (AGA Gas) was added in order to reduce the intensity of S_2 transitions near the frequency of the rare gas complex transitions.[26] The mixture of H_2S, rare-gas,

 © 1998 American Institute of Physics

This article is copyrighted as indicated in the article. Reuse of AIP content is subject to the terms at: http://scitation.aip.org/termsconditions. Downloaded to IP: 193.0.65.67 On: Sat, 29 Nov 2014 12:28:31

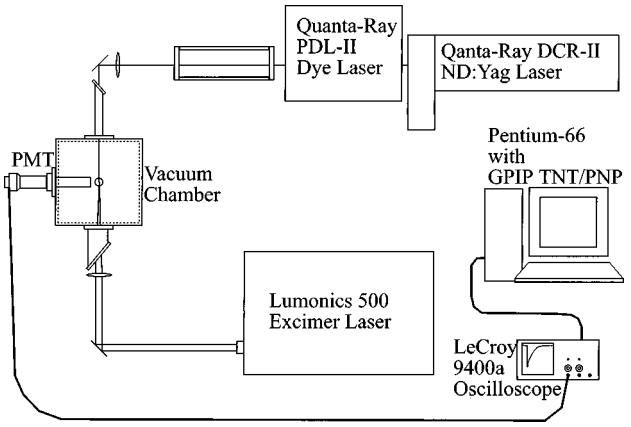

FIG. 1. Schematic of experimental apparatus.

and He was produced via a system of needle valves at a stagnation pressure of 75-125 psi before being expanded through the pulsed valve.

To ensure that the $\tilde{A}$ state molecules in the free jet were not undergoing collisional relaxation to lower vibrational states before emission we varied the conditions of the expansion. We changed the stagnation pressure from 75–125 psi and varied the distance between the pulsed valve and probe beam from 44–134 nozzle diameters. No change in the natural lifetime was observed for any combination of these parameters. We therefore conclude that we are operating in a region of the free jet expansion where collisional relaxation is negligible.

A typical experimental temporal decay for a given vibrational level of the $\tilde{A}\ ^2\Sigma^+$ state of the R·SH complexes was collected in the following manner. After optimizing the signal of the transition the experiment was set up to acquire 10 decay curves programatically, each averaged over 1000 shots. Then one more trace was collected with the dye laser detuned from the transition, again averaged over 1000 shots. This trace served as a background to be subtracted from the other ten traces. This allowed us to remove the background fluorescence present from the emission of higher clusters, $R_n \cdot SH$ where $n \geqslant 4$ and any scattered light from the photolysis or probe lasers. Additionally for transitions in which the signal to noise ratio was great enough the collection optics were removed and the above procedure was again followed. This allowed us to observe the effect of molecules leaving the light collection region before emitting.

III. DATA ANALYSIS

The intensity, I, of radiation reaching our detector as a function of time, can be written as

$$I = I_0 e^{-t/\tau_{\text{obs}}} + I_B, \tag{1}$$

where $I_0 = I$ evaluated at $t = 0$, $t =$ time after the excitation laser pulse, $\tau_{\text{obs}} =$ observed lifetime, $I_B =$ intensity of any background radiation (experimentally determined to be time independent).

Our experimentally obtained decay curves are fit to Eq. (1), allowing I_0, I_B, and τ_{obs} to vary. Often similar fits have been performed by noting that the ln $(I - I_B)$ vs t yields a straight line with slope τ_{obs}^{-1}. Under circumstances in which there is little contribution to the temporal decay by molecules leaving the light collection region before emitting, the signal to noise is good, and the magnitude of the background fluorescence signal is small compared to the R·SH signal, fitting either form of the equation yields equivalent values for τ. However, when any of the above conditions are not met we have found that fitting Eq. (1) itself is more reliable and with modern computer techniques as straightforward. For this reason all data were fit to Eq. (1).

Actual fitting of the data was done using the fitting capabilities of the program Sigma Plot 4.0. For each trace the data was trimmed to the middle 80%, i.e., the first 10% of the decay curve and the last 10% were deleted. Each trace was then fit to Eq. (1). The results of ten fits were then averaged.

For transitions which exhibited long lifetimes ($\tau_{\text{obs}} \geqslant 500$ ns) it was noted that data taken without the collection optics produced values of τ_{obs} significantly longer than those obtained with the optics in place. This indicates that in some cases a non-negligible number of molecules leave the light collection region before fluorescing. Given the significant effect of the collection optics and the fact that we were not able to omit the optics for all transitions of interest because the light intensity was too low, we need to correct our data for this effect.

As a first approximation we assume the rates of the two effects are additive;

$$\frac{1}{\tau_{\text{nat}}} = \frac{1}{\tau_{\text{obs}}} - \frac{1}{\tau_c}, \tag{2}$$

where τ_{nat} is the actual natural lifetime, τ_{obs} is the experimentally observed lifetime, and τ_c is the correction factor. The correction factor is determined by assuming that the lifetime values obtained without the collection optics are equal to τ_{nat} and the lifetime values obtained with the collection optics are equal to τ_{obs} in Eq. (2).

The average values for τ_c for the Ne, Ar, and Kr complexes are 20778 ns, 3195 ns and 9212 ns, respectively. The τ_c value for Ne is as large as it is because Ne comprises a much higher percentage of the expansion than either Ar or Kr, hence the velocity of the expansion is slowed considerably from that for pure He. The values for the Ne, Ar, and Kr seeded expansion are all roughly consistent with the expected velocity ratios calculated for the mixtures with He that were employed.

The errors reported for the lifetime measurements for the Ar and Kr complexes are two standard deviations as calculated for the group of ten measurements made for each transition. For the Ne·SD complex the error reported corresponds to one standard deviation. The reason for the difference in calculating error limits arises from the greater difficulty in measuring a good baseline for the case of Ar and Kr complexes. In Ar and Kr where there is significant background fluorescence from larger clusters, the baseline fluctuates a great deal for a relatively small change in the concentration of the rare gas. This effect was minimized to the point that it did not make much difference for a single set of ten traces, however when revisiting the same transition and ac-

This article is copyrighted as indicated in the article. Reuse of AIP content is subject to the terms at: http://scitation.aip.org/termsconditions. Downloaded to IP: 193.0.65.67 On: Sat, 29 Nov 2014 12:28:31

TABLE I. Comparison of radiative lifetimes.

Method	SH	SD
osc. strengths[a]	820(240)	730(180)
ab initio[b]	704	688
Kr matrix[c]	800	d
present work	820(50)	810(30)[e]

[a]Determined by absolute concentration calibrations of SH and SD in a fast flow reactor and fluorescence measurements, by Friedl *et al.* (Ref. 14).
[b]Derived from *ab initio* calculations by Senekowitsch *et al.* (Ref. 27).
[c]From fit of temporal decays in Kr matrix, corrected for Stokes shifts and for change in dielectric medium, by Zoval *et al.* (Ref. 24).
[d]No data are available for SD in a rare gas matrix.
[e]This number is arrived at by averaging all of the levels considered to be totally trapped in Kr·SD and Ar·SD.

quiring another ten traces we found that the data would typically vary somewhat more than one standard deviation. Therefore we have adopted two standard deviations as our error limits which was sufficient to encompass all of the data that was acquired. In the case of Ne·SD there was no background fluorescence and one standard deviation was sufficient to encompass the observations.

IV. RESULTS AND DISCUSSION

A. Radiative lifetimes

It is useful to compare our results to the radiative lifetimes observed for the bare SH/D and SH in Kr and Ar matrices. These are summarized in Table I. In our experiments the radiative lifetimes were determined by taking the average of all levels considered to be totally trapped for a given complex. The transitions included in the average for each complex are marked in Tables II and III. Overall we obtain a radiative lifetime of 820(50) ns for SH and 810(30) ns for SD. The isotopomer values are, as expected, within experimental error.

Although we would not expect the radiative lifetimes of bare SH/D to be exactly identical to that of the rare gas

TABLE II. Natural lifetimes of R·SH.

R	$\tilde{A}\ ^2\Sigma^+$ vibrational level[a]	$\tilde{X}\leftarrow\tilde{A}$ transition (cm^{-1})[b]	τ_{nat}(ns)[c] expt	P_{out}	τ_{nat}(ns)[d] calc
Kr	$(0,0^0,8)$	30507.57(1)	630(30)	0.016	660(35)
	$(0,0^0,9)$	30579.78(1)	530(30)	0.028	495(20)
	$(0,0^0,10)$	30646.47(1)	310(30)	0.043	314(7)
	$(0,0^0,11)$	30706.10(1)	140(30)	0.068	174(2)
	$(0,0^0,12)$	30759(2)	80(20)	0.11	83.7(0.5)
	$(0,1^1,6)$	30590(2)	450(30)	0.061	430(15)
	$(0,1^1,7)$	30664.75(5)	210(30)	0.091	240(4)
	$(0,1^1,8)$	30727.32(5)	90(20)	0.15	106.5(0.8)
	$(0,2^0,2)$	30504(2)	600(30)	0.044	610(30)
	$(0,2^0,4)$	30674(2)	160(20)	0.15	150(2)
Ar	$(0,0^0,0)$[e]	30457(2)	820(50)	0.0042	800(45)
	$(0,0^0,1)$	30536.69(1)	790(40)	0.010	735(40)
	$(0,0^0,2)$	30609.09(1)	630(30)	0.022	590(25)
	$(0,0^0,3)$	30673.55(1)	370(30)	0.043	380(10)
	$(0,0^0,4)$	30730.38(1)	150(30)	0.081	198(3)
	$(0,0^0,5)$	30779.81(1)	90(20)	0.17	82.4(0.5)
	$(0,1^1,1)$	30735.9(1)	150(30)	0.12	193(3)
	$(0,1^1,2)$	30787.58(1)	60(20)	0.26	73.9(0.4)
Ne[f]	$(0,0^0,0)$		$\leqslant 20$	0.42	6.7

[a]The quantum numbers used to describe these complexes are (ν_{SH},ν_b^k,ν_s) where nominally ν_{SH} is the SH monomer stretch, ν_b^k is the bending mode, and ν_s is the R-SH stretch.
[b]Quoted frequencies obtained from Carter *et al.* (Ref. 26).
[c]In the case when both corrected lifetimes and lifetimes taken without collection optics were available an average of the two is quoted.
[d]Theoretical lifetimes were calculated by McCoy (Ref. 25) using the ballistic model.
[e]Vibrational level used to calculate τ_{rad}.
[f]A number of higher vibrational levels were experimentally examined and all had $\tau \leqslant 20$ ns. Calculated τ's were all <10 ns.

This article is copyrighted as indicated in the article. Reuse of AIP content is subject to the terms at: http://scitation.aip.org/termsconditions. Downloaded to IP: 193.0.65.67 On: Sat, 29 Nov 2014 12:28:31

TABLE III. Natural lifetimes of R·SD.

R	$\tilde{A}\ ^2\Sigma^+$ vibrational level[a]	$\tilde{X}\leftarrow\tilde{A}$ transition (cm^{-1})[b]	τ_{nat} (ns)[c] expt	P_{out}	τ_{nat} (ns)[d] calc
Kr	$(0,0^0,8)$[e]	30549.6(1)	810(40)	0.0030	810(30)
	$(0,0^0,9)$[e]	30625.6(1)	800(40)	0.0059	810(30)
	$(0,0^0,10)$[e]	30698.8(1)	820(30)	0.012	805(30)
	$(0,0^0,11)$[e]	30765.5(1)	810(30)	0.22	800(30)
	$(0,0^0,12)$[e]	30825(2)	840(30)	0.040	790(30)
	$(0,0^0,13)$[e]	30880(2)	820(30)	0.067	765(25)
	$(0,0^0,14)$[e]	30927(2)	800(40)	0.12	705(25)
	$(0,1^1,8)$[e]	30721(2)	840(50)	0.32	805(30)
	$(0,1^1,9)$[e]	30788(2)	810(30)	0.63	795(30)
	$(0,1^1,10)$[e]	30849(2)	830(30)	0.11	765(30)
	$(0,1^1,11)$	30902(2)	770(30)	0.17	710(25)
Ar	$(0,0^0,3)$[e]	30738.21(2)	770(50)	0.010	810(30)
	$(0,0^0,4)$[e]	30800.01(2)	790(30)	0.022	805(30)
	$(0,0^0,5)$	30855.2(1)	760(30)	0.053	790(28)
	$(0,0^0,6)$	30902(3)	750(30)	0.12	750(25)
	$(0,1^1\ [2^2],2[0])$[e,f]	30812(5)	790(50)	0.061[0.087][f]	800(30)[795(30)][f]
	$(0,1^1\ [2^2],3[1])$[f]	30868(5)	760(30)	0.14[0.20][f]	770(30)[755(25)][f]
	$(0,1^1\ [2^2],4[2])$[f]	30917(5)	650(50)	0.40[0.40][f]	665(20)[670(20)][f]
Ne	$(0,0^0,0)$	30931.4(1)	491(10)	0.19	420(8)
	$(0,0^0,1)$	30961(5)	301(15)	0.42	301(4)
	$(0,1^0,0)$	30943(5)	337(15)[g]	0.85	226(2)
	$(0,1^1,0)$	30954(5)	290(30)[h]	0.71	226(2)
	$(0,2^k,0)$	30979(5)	289(15)		
Ne_n, $n\geqslant 2$		30885(5)	672(15)		
		30895(5)	670(10)		
		30898(5)	651(10)		
		30904(5)	648(10)		
		30917(5)	612(10)		

[a]The quantum numbers used to describe these complexes are (ν_{SH},ν_b^k,ν_s) where nominally ν_{SH} is the SH monomer stretch, ν_b^k is the bending mode, and ν_s is the R-SH stretch.

[b]Quoted frequencies for Kr and Ar complexes obtained from Carter *et al.* (Ref. 26) and Yang *et al.* (Ref. 10). Quoted frequencies for Ne complexes were calibrated relative to the frequency of the $(0,0^0,0)$ band of Ne·SD quoted by Carter *et al.* (Ref. 26).

[c]In the case when both corrected lifetimes and lifetimes taken without collection optics were available an average of the two is quoted.

[d]Theoretical lifetimes were calculated by McCoy (Ref. 25) using the ballistic model.

[e]Vibrational level used to calculate τ_{rad}.

[f]The assignments in brackets are alternative assignments to those outside the brackets. The bands observed is this progression may either be a blend of both bands or an individual broad band. The lack of high resolution data makes it impossible to make a unique assignment. The assignment was based purely on the calculations of Korambath *et al.* (Ref. 11). The τ_{calc} and P_{out} in brackets corresponds to the calculated values for the assignments in brackets.

[g]Lifetime corrected for overlap with a Ne_nSD vibrational level with a lifetime of 520 ns.

[h]Lifetime corrected for overlap with a SD rotational level with a lifetime of 190 ns.

complexes, we would expect that the perturbation caused by the addition of the rare gas atom to be small. This is born out by a comparison to the data obtained by Friedl *et al.*[14] on SH/D in a fast flow reactor. For SH we see that the Ar·SH radiative lifetime yields the same value as that observed by Friedl *et al.*,[14] but with considerably less error. For the Kr·SH complex none of the observed vibrational levels appear to be completely trapped. In the case of SD a comparison of its radiative lifetime to that of the Kr and Ar complexes shows a somewhat higher radiative lifetimes for the

This article is copyrighted as indicated in the article. Reuse of AIP content is subject to the terms at: http://scitation.aip.org/termsconditions. Downloaded to IP: 193.0.65.67 On: Sat, 29 Nov 2014 12:28:31

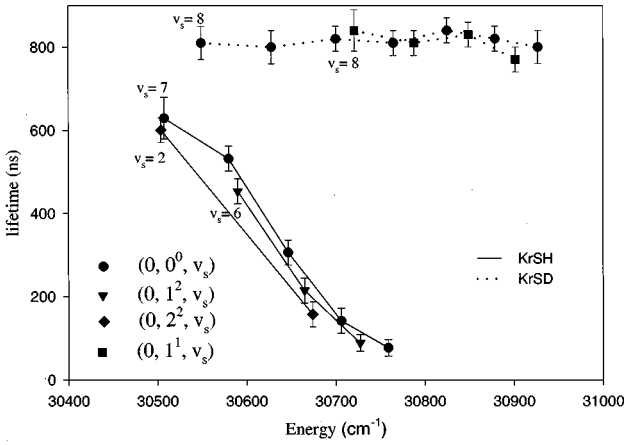

FIG. 2. Plots of lifetimes vs energy for Kr·SH/D. The quantum numbers used to describe these complexes are $(\nu_{SH}, \nu_b^k, \nu_s)$ where nominally ν_{SH} is the SH monomer stretch, ν_b^k is the bending mode, and ν_s is the R-SH stretch. The value of ν_s is given on the plot for the lowest frequency member of a progression with a given value of ν_b^k. Sequential points to higher energy increase ν_s by one. Energy is measured with respect to the vibrationless level of the $\tilde{X}$ state.

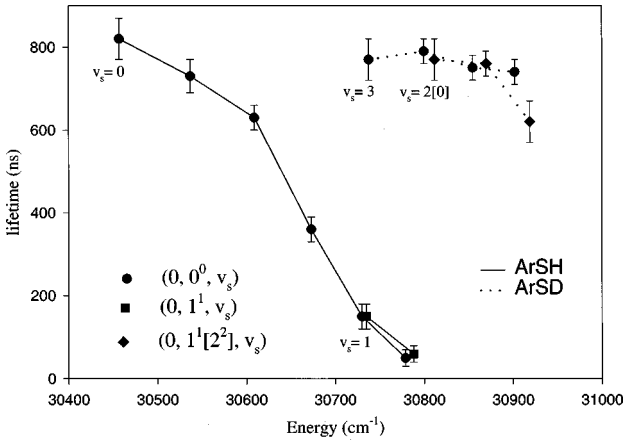

FIG. 3. Plots of lifetimes vs energy for Ar·SH/D. The quantum numbers used to describe these complexes are $(\nu_{SH}, \nu_b^k, \nu_s)$ where nominally ν_{SH} is the SH monomer stretch, ν_b^k is the bending mode, and ν_s is the R-SH stretch. The value of ν_s is given on the plot for the lowest frequency member of a progression with a given value of ν_b^k. Sequential points to higher energy increase ν_s by one. Energy is measured with respect to the vibrationless level of the $\tilde{X}$ state. The assignments in brackets are alternative assignments to those outside the brackets. The bands observed in this progression may either be a blend of both bands or an individual broad band. The lack of high resolution data makes it impossible to make a unique assignment. The assignment was based purely on the calculations of Korambath, *et al.* (Ref. 11).

complexes, but still within experimental error of Friedl *et al.*[14] A comparison to the *ab initio* calculations of Senekowitsch *et al.*[27] shows the observed radiative lifetimes to be considerably higher than that of both SH and SD. However Senekowitsch *et al.*[27] noted that these calculated lifetimes may be somewhat too short, because of difficulties in calculating the transition moments. Useful comparisons to the data obtained by Aparkian *et al.*[24] in Kr and Ar matrices may also be made, however in there experiment only data for SH was obtained. The radiative lifetime determined for SH in a Kr matrix agrees well with the radiative lifetime presently determined. The observations of the radiative lifetime of SH in an Ar matrix are substantially lower than those in the Kr matrix and those observed for the Ar·SH complex in this work. This may indicate that the dissociation of the SH moiety is inhibited in the Ar matrix, but perhaps not entirely arrested. For this reason the radiative lifetime of SH determined in the Ar matrix is not included in Table I.

B. Experimental lifetime trends for complexes

A summary of the experimental data for all the observed vibrational levels of the $\tilde{A}$ state of the R·SH complexes is found in Tables II and III. Additionally, plots of lifetime vs relative energy are provided in Figs. 2, 3, and 4. The analyses of the data for the complexes will be discussed in order of decreasing size of the rare gas complexes (i.e., Kr, Ar, Ne).

For the Kr·SH and Ar·SH complexes we see from Table II and Figs. 2 and 3 that there is a gradual decrease in lifetime as we increase the amount of vibrational energy in the complex. We see in the Kr·SH data that the addition of a quantum of bend somewhat increases the probability of dissociation at lower energies; hence energy placed in the bending mode is more efficient at promoting dissociation than equivalent energy placed in the stretching mode.

The bend-stretch data for Ar·SH is somewhat sparse. However for this complex the addition of a bend to the stretch appears to cause only a small increase in the decay rate. It is probably that in these levels of Ar·SH that we are already sufficiently near the predissociative lifetime limit, so that any increase in decay rate must be slight.

The data for the deuterated species of Kr and Ar complexes show a quite different behavior to that of the nondeuterated species. It appears that deuterium substitution completely quenches the fragmentation process for most levels.

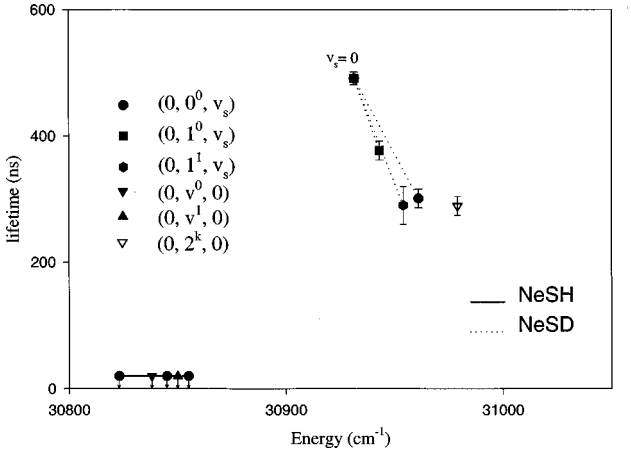

FIG. 4. Plot of lifetimes vs energy for Ne·SH/D. The quantum numbers used to describe these complexes are $(\nu_{SH}, \nu_b^k, \nu_s)$ where nominally ν_{SH} is the SH monomer stretch, ν_b^k is the bending mode, and ν_s is the R-SH stretch. The value of ν_s is given on the plot for the lowest frequency member of a progression with a given value of ν_b^k. Sequential points to higher energy increase ν_s by one. Energy is measured with respect to the vibrationless level of the $\tilde{X}$ state.

This article is copyrighted as indicated in the article. Reuse of AIP content is subject to the terms at: http://scitation.aip.org/termsconditions. Downloaded to IP: 193.0.65.67 On: Sat, 29 Nov 2014 12:28:31

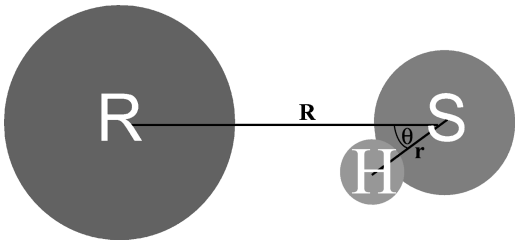

FIG. 5. Model of the geometry of R·SH where R is the rare gas atom, S is the sulfur atom, H is the hydrogen atom, **R** is the axis which connects the rare gas atom and the center of mass of the SH moiety, **r** is the bond distance of the SH moiety, and θ is the angle between **R** and **r**. This model also applies to R·SD with obvious modifications.

Indeed the only significant decrease in lifetime occurs after one quantum of bending motion is added to a complex.

The lifetimes in Ne·SH are all sufficiently short that their observed decay rates are all instrumentally limited. Thus we can only provide an upper limit of 20 ns for them. Clearly, the Ne atom is not able to effectively block the dissociation of SH and the escape of H. On the other hand Ne is significantly more effective in the Ne·SD complex at blocking the deuterium atom from dissociating. Particularly at the origin we see significant lengthening of the complexes lifetime compared to free SH/D.

C. A simple model

Figure 5 shows a ''billiard ball'' classical picture of the geometry of the R·SH complexes. Figure 5 also serves to define the distance R between the two moieties in the complex and the angle θ which the SH/D bond makes with the axis determined by the centers of mass of the moieties. In Fig. 6(a) we show a reasonable representation of the $X\ ^2\Pi$, $A\ ^2\Sigma^+$ and $a\ ^4\Sigma^-$ potential curves for the isolated SH/D radical. We also expect that Fig. 6(a) represents a fairly good approximation for the corresponding $\tilde{X}$, $\tilde{A}$, and $\tilde{a}$ states of the complex, if it is interpreted as one of many cuts through the surface corresponding to fairly large R or for moderate R and/or $\theta \gtrsim \pi/4$, or a reasonable combination thereof. On the other hand Fig. 6(b) can be thought of as a reasonable representation of these curves for moderate to short R and/or $\theta \approx 0$ or a reasonable combination thereof. Figure 6(b) differs from Fig. 6(a) in that there are large potential barriers present in each of the $\tilde{X}$, $\tilde{A}$, and $\tilde{a}$ states due to the presence of the inert gas atoms.

Obviously when the S–H/D bond breaks almost all the atomic motion is centered in the H/D while the heavy S and R atoms remain nearly stationary. Then the potential barriers of Fig. 6(b) which effectively prevent dissociation along the S–H bond correspond in the classical picture to the H atom ''crashing'' into the rare gas and its escape thereby being prevented.

In an accompanying paper, McCoy[25] has developed both the classical and quantum mechanical picture in considerable detail, and is able to make predictions with both models, that replicate our observations with considerable accuracy. We recommend this paper to the reader.

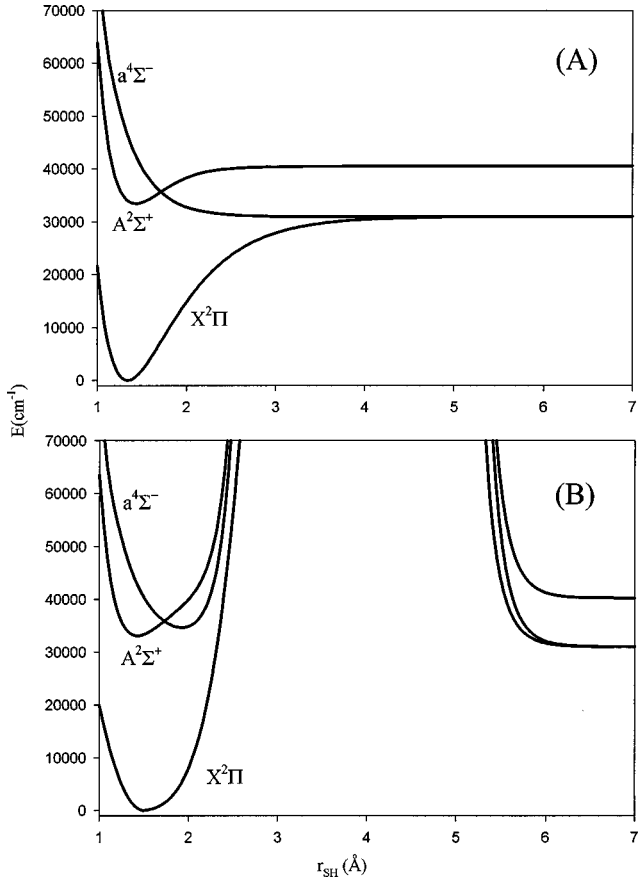

FIG. 6. (a) $X\ ^2\Pi$, $A\ ^2\Sigma^+$, and $a\ ^4\Sigma^-$ potential curves for the isolated SH/D radical which correspond to cuts of the R·SH/D complex's potential surface for fairly large R as well as for moderate R with $\theta \gtrsim (\pi/4)$ or a reasonable combination thereof. (b) Corresponding cuts of the R·SH/D potential surfaces, but for fairly short R or moderate R with $\theta \approx 0$ or a reasonable combination thereof.

In our present effort to interpret our experimental results, we will confine ourselves to the classical model, but note that there is a close correspondence between it and the more quantum mechanical description. The classical model yields zero probability for dissociation for certain combinations of R and θ, such that $R \sin\theta \leqslant \rho_n$, where ρ_n is the sum of the H and R van der Waals radii while allowing it to proceed at the free SH rate for all other combinations of R and θ values. This corresponds to assuming the surfaces in Fig. 6 are characterized by a barrier with zero transmission coefficient for R, θ cuts for which $R \sin\theta \leqslant \rho_n$ and zero barrier otherwise. With this model it immediately follows that

$$\tau_{\text{nat}}^{-1} = \tau_R^{-1} + \alpha \tau_F^{-1}, \tag{3}$$

with

$$\tau_{\text{F}}^{-1} = \tau_{\text{SH/D}}^{-1} P_{\text{out}}, \tag{4}$$

where τ_R^{-1}= radiative decay rate (assumed the same for R·SH/D and free SH/D, see Table I), τ_F^{-1}= fragmentation rate, α= correction factor, $\tau_{\text{SH/D}}^{-1}$= fragmentation rate of free SH/D, P_{out}= probability, for a particular vibrational level of the complex, that $R \sin\theta > \rho_n$. Numerical values for the $\tau_{\text{SH/D}}$'s for isolated SH/D are taken from the literature[14] as $\tau_{\text{SH}} = 3(2)$ ns and $\tau_{\text{SD}} = 260(100)$ ns.

This article is copyrighted as indicated in the article. Reuse of AIP content is subject to the terms at: http://scitation.aip.org/termsconditions. Downloaded to IP: 193.0.65.67 On: Sat, 29 Nov 2014 12:28:31

While this model is simple and relies principally upon measured parameters for the isolated radical, for most molecular complexes its predictive power for the observed lifetimes would be severely limited. This limitation arises because of lack of knowledge of P_{out}. However in the case of the R·SH we are very fortunate. In recent papers[11,28] we have described detailed calculations of all the observed eigenvalues and their corresponding eigenfunctions based upon an empirically determined potential. P_{out} is simply and, we believe, rather accurately calculated from the square of the vibrational eigenfunctions of R and θ, for values of $R \sin\theta > \rho_n$.

In Tables I and II, we include the results for P_{out} for each observed vibrational level in Table I. One may note that such a calculation contains no adjustable parameters and is based upon the obviously rather crude assumption that at a given R and θ value the probability for fragmentation in the complex can have only two values, 0 and $\tau_{\text{SH/D}}^{-1}$. While this calculation gives good qualitative results, its quantitative predictive power can be greatly increased by adjusting the predicted τ_F by a multiplicative factor α, where

$$\alpha = e^{-\beta(D_0 - E_n)}, \tag{5}$$

with D_0 the dissociation energy of the rare gas complex and E_n the energy of the vibrational level above the vibrationless one. As pointed out by McCoy β can be optimized once for the pure stretch levels, $\beta_0 = 0.00659$ cm, and once for levels containing bending motion, $\beta_1 = 0.00811$ cm. The physical justification for this factor is the clear recognition that complexation with the inert gas causes the potential curves to shift with respect to one another which means that even where $R \sin\theta > \rho_n$, τ^{-1} is not quite $\tau_{\text{SH/D}}^{-1}$ of the free SH/D radical.

D. Comparison of experimental results with model

Tables II and III compare for R·SH and R·SD respectively the experimentally observed lifetimes, τ_{nat}, with those predicted from the model via Eqs. (3) and (4). It is worthwhile noting that in the absence of an inert gas, SH molecules excited to the $v=0$ of the $A\ ^2\Sigma^+$ state decay predominately (>99%) by fragmentation, i.e., $\tau_{\text{nat}}/\tau_{\text{rad}} \lesssim 0.01$. Looking first at the stretch levels $(0,0^0,v_s)$ of Kr·SH we note that the lowest observed level is fairly highly excited with $v_s = 7$. Yet we see that complexation with the Kr atom even at this large R reduces the fragmentation percentage to only about 25% compared to greater than 99% in the free molecule. Table II shows that because of the rather tight anisotropic bending in this complex the H atom spends most of its time $(1 - P_{\text{out}})$ in the ''shadow'' of the Kr atom. As v_s increases, so does P_{out}, thereby significantly decreasing the probability that the H atom is in the shadow of the Kr. As Table II shows there is good agreement between the observed decrease in τ_{nat} compared to the predictions.

Table II also quite clearly shows how for a given v_s, P_{out} is increased by adding one quanta of bending excitation to the complex for $v_s = 7$ and 8. Clearly this increases the probability that the H is out of the shadow of the Kr and this is reflected by the observed decrease in the lifetimes by roughly a factor of 7. Table II shows that overall the model predicts these trends quite well.

Turning to Table III we see that for all the stretching levels in Kr·SD, including excitation up to $v_s = 13$, τ_{nat} is essentially constant at the value of τ_{rad}. Similarly, when we add one quantum of bend to the stretching mode we again observe τ_{nat} essentially constant at the value of τ_{rad}. Only when we get to $v_s = 11$ in the bend-stretch combination do we see a slight decrease in lifetime. The model does an excellent job of predicting these observations. Equation 4 shows that this differential ''trapping'' between isotopomers is really caused by two effects. First P_{out} is considerably smaller in the deuteride because its amplitude of vibration is considerably less. In addition $\tau_{\text{SD}} \gg \tau_{\text{SH}}$ in the free molecule presumably due to a shift of the curve crossing relative to the $v=0$ level.

Turning to the Ar·SH complex we see from Table II that for the vibrationless level photofragmentation is essentially eliminated yielding the radiative lifetime. However when 5 quanta of v_s are added to the complex about 95% of the molecules photofragment. This trend is again well predicted by the simple model. Likewise we see that for a given stretch level, addition of one quantum of bend decreases τ_{nat} by a factor of 5-10. Obviously again P_{out} is dramatically increased and the model well predicts the trend.

When we consider the deutride complex, Ar·SD, we see a result quite similar to Kr·SD where photofragmentation was completely arrested. For the Ar complex, all but a couple of levels show τ_{nat} within 20% of τ_{rad}. Only when significant amounts of bending excitation, e.g., $(0,1^1,4)$ and $(0,2^0,2)$ are involved are significant deviations from τ_{rad} observed. In all cases Tables II and III show that the model adequately predicts the observations.

For the Ne·SH complex all observed levels decay with lifetimes ($\tau_{\text{nat}} \lesssim 20$ ns) below instrumental resolution. Because of the large amplitude vibrations in this weakly bound complex, P_{out} for all these states is large and the model predicts lifetimes 10 ns for all of the observed levels, well below experimental resolution. Interestingly τ_{nat} for Ne·SD is much longer and easily measured as shown in Table III. As Eq. (4) shows, qualitatively this effect arises, as in Ar·SD from the dual factors of P_{out} and τ_{SD}^{-1} decreasing compared to the hydride complex. This trend is also predicted by the model.

V. CONCLUSIONS

Lifetime data for a large number of vibronic levels of the $\tilde{A}\ ^2\Sigma^+$ state of the R·SH/D (R=Ne, Ar and Kr) has been gathered. From this data we are able to establish a radiative lifetime of the monomer species of 820(50) ns for SH and 810(30) ns for SD. We have explained the observed, natural lifetime variations by a factor of up to ≈100 in the complexes in terms of a classical picture of the dynamics. This model treats the atoms as solid spheres and assumes that the photofragmentation channel is only available if the H/D atom lies outside the shadow of the inert gas. This model successfully explains a number of observed trends including

This article is copyrighted as indicated in the article. Reuse of AIP content is subject to the terms at: http://scitation.aip.org/termsconditions. Downloaded to IP: 193.0.65.67 On: Sat, 29 Nov 2014 12:28:31

the gradual decrease seen in the lifetimes in the Kr·SH and Ar·SH species. It also accounts for the somewhat surprising, nearly constant, lifetime observed in the deuterides. It accounts for a very short τ_{nat} for Ne·SH where we are only able to establish an upper limit to the natural lifetime as 20 ns, but predicts for the Ne·SD species the experimentally observed trend which is similar to that of Kr·SH and Ar·SH.

ACKNOWLEDGMENTS

The authors acknowledge the support of this work via NSF Grant No. CHE 9320909. We thank Anne McCoy for many useful discussions and access to the results of her calculations (quoted herein) prior to publication.

[1] J. C. Polanyi and A. H. Zewail, Acc. Chem. Res. **28**, 119 (1995).
[2] S. S. Brown, R. B. Metz, H. L. Berghout, and F. F. Crim, J. Chem. Phys. **105**, 6293 (1996).
[3] D. Bingemann, M. P. Gorman, A. M. King, and F. F. Crim, J. Chem. Phys. **107**, 661 (1997).
[4] R. D. Guettler, G. C. Jones Jr., L. A. Posey, and R. N. Zare, Science **266**, 259 (1994).
[5] D. E. Powers, M. Pushkarsky, and T. A. Miller, J. Chem. Phys. **106**, 6863 (1997).
[6] D. E. Powers, M. B. Pushkarsky, M. C. Yang, and T. A. Miller, J. Phys. Chem. **101**, 9846 (1997).
[7] D. C. Sorenson, SIAM J. Matrix Anal. Appl. **13**, 357 (1992).
[8] S. E. Choi and J. C. Light, J. Chem. Phys. **97**, 7031 (1992).
[9] P. P. Korambath, X. T. Wu, and E. F. Hayes, J. Phys. Chem. **100**, 6116 (1996).
[10] M. C. Yang, C. C. Carter, and T. A. Miller, J. Chem. Phys. **107**, 3437 (1997).
[11] P. P. Korambath, W. T. Wu, E. F. Hayes, C. C. Carter, and T. A. Miller, J. Chem. Phys. **107**, 3460 (1997).
[12] W. Ubachs, J. Ter Muelen, and A. Dymanus, Chem. Phys. Lett. **101**, 1 (1983).
[13] J. Tiee, M. Ferris, and F. B. Wampler, J. Chem. Phys. **79**, 130 (1983).
[14] R. R. Friedl, W. H. Brune, and J. G. Anderson, J. Chem. Phys. **79**, 4227 (1983).
[15] M. Kawasaki, H. Sato, G. Inoue, and M. Suzuki J. Chem. Phys. **91**, 6758 (1989).
[16] S. Fei, X. Zheng, and M. C. Heaven, J. Chem. Phys. **97**, 1655 (1992).
[17] Y. Lin, S. Fei, X. Zheng, and M. C. Heaven, J. Chem. Phys. **96**, 5020 (1992).
[18] S. Lin, K. Kulkarni, and M. C. Heaven, J. Chem. Phys. **94**, 1720 (1990).
[19] C.-C. Chuang, P. M. Andrews, and M. I. Lester, J. Chem. Phys. **103**, 3418 (1995).
[20] J. J. Valenti and J. B. Cross, J. Chem. Phys. **77**, 572 (1982).
[21] J. A. Beswick, R. Monot, J.-M. Philippoz, and H. van den Bergh, J. Chem. Phys. **86**, 3965 (1987).
[22] C. Wan, M. Gupta, J. S. Baskin, Z. H. Kim, and A. H. Zewail, J. Chem. Phys. **106**, 4353 (1997).
[23] M.-C. Yang, A. P. Salzberg, B.-C. Chang, C. C. Carter, and T. A. Miller, J. Chem. Phys. **98**, 4301 (1993).
[24] J. Zoval, D. Imre, and V. A. Apkarian, J. Chem. Phys. **98**, 1 (1993).
[25] A. McCoy, J. Chem. Phys. **109**, 170 (1998), following paper.
[26] C. C. Carter and T. A. Miller, J. Chem. Phys. **107**, 3447 (1997).
[27] J. Senekowitsch, H.-J. Werner, P. Rosmus, and E. Reinsch, J. Chem. Phys. **83**, 4661 (1985).
[28] M. C. Yang, J. M. Williamson, and T. A. Miller, J. Mol. Spectrosc. **107**, 3437 (1997).

This article is copyrighted as indicated in the article. Reuse of AIP content is subject to the terms at: http://scitation.aip.org/termsconditions. Downloaded to IP: 193.0.65.67 On: Sat, 29 Nov 2014 12:28:31